PNAS RESEARCH ARTICLE | MEDICAL SCIENCES

Pharmacological inhibition of HIF2 protects against bone loss in an experimental model of estrogen deficiency

Giulia Lanzolla[a,1], Elena Sabini[a,1], Katherine Beigel[b], Mohd Parvez Khan[a], Xiaowei Sherry Liu[a], Dian Wang[a], Brittany Laslow[a], Deanne Taylor[b], Teresita Bellido[c,d], Amato Giaccia[e], and Ernestina Schipani[a,2]

Edited by Sundeep Khosla, Mayo Clinic Alix School of Medicine, Rochester, Minnesota; received August 23, 2024; accepted November 2, 2024 by Editorial Board Member Natalie G. Ahn

Estrogen deficiency, which is linked to various pathological conditions such as primary ovarian insufficiency and postmenopausal osteoporosis, disrupts the delicate balance between bone formation and resorption. This imbalance leads to bone loss and an increased risk of fractures, primarily due to a significant reduction in trabecular bone mass. Trabecular osteoblasts, the cells responsible for bone formation within the trabecular compartment, originate from skeletal progenitors located in the bone marrow. The microenvironment of the bone marrow contains hypoxic (low oxygen) regions, and the hypoxia-inducible factor-2α (HIF2) plays a crucial role in cellular responses to these low-oxygen conditions. This study demonstrates that the loss of HIF2 in skeletal progenitors and their derivatives during development enhances trabecular bone mass by promoting bone formation. More importantly, PT2399, a small molecule that specifically inhibits HIF2, effectively prevents trabecular bone loss in ovariectomized adult mice, a model for estrogen-deficient bone loss. Both the genetic and pharmacological approaches result in an increase in osteoblast number, which is linked to the expansion of the pool of skeletal progenitor cells. This expansion either by loss or inhibition of HIF2 uncovers a pivotal mechanism for increasing osteoblast numbers and bone formation, resulting in greater trabecular bone mass.

hypoxia | hIF2 | PT2399 | osteoporosis | osteoblasts

Significance

hypoxia-inducible factor-2α (HIF2) is a negative regulator of bone mass accrual. Here, we establish that the pharmacological inhibition of HIF2 is sufficient to prevent bone loss upon ovariectomy primarily through enhanced bone formation. These findings support further investigations of HIF2 inhibitors as agents to treat loss of bone mass due to estrogen deficiency.

The development of new treatments for low-bone mass diseases, such as postmenopausal osteoporosis, is a highly active field of investigation. Osteoporosis is a systemic skeletal disease characterized by low bone mass and microarchitectural deterioration of bone tissue (1). It impacts over 20 million Americans and results in approximately 1.5 million "fragility" fractures annually (2, 3). In addition to postmenopausal osteoporosis, other conditions linked to estrogen deficiency such as primary ovarian insufficiency, which occurs in younger subjects, can also result in bone loss and fragility (4, 5).

Adult bone undergoes continuous remodeling throughout life, accomplished by two specialized cell types: bone-resorbing osteoclasts and bone-forming osteoblasts (6). The activity of osteoblasts is coupled with that of osteoclasts, allowing for the maintenance of bone and mineral homeostasis in adulthood (7). Estrogens play a key role in bone metabolism and remodeling, acting on both osteoblasts and osteoclasts (8, 9). Estrogen deficiency leads to an imbalance between bone formation and resorption either directly or indirectly through the regulation of hormones such as follicle-stimulating hormone (10, 11).

The various conditions associated with estrogen deficiency may require tailored treatments customized to patients as the degree of bone loss depends on the underlying condition and the timing of analysis. Current treatments for postmenopausal osteoporosis include antiresorptive drugs and agents that promote bone formation, such as parathyroid hormone (PTH), PTH-related protein (PTHrP) analogs, and monoclonal antibodies against sclerostin (12, 13). While these treatments are effective for high-risk patients, their prolonged use is associated with significant side effects that lead to their discontinuation (13, 14). Additionally, in contrast to anti-sclerostin antibodies which also reduce Bone Resorption, PTH and PTHrP analogs tend to increase Bone Resorption over time, diminishing their overall anabolic benefits (15).

Although several options exist for treating established bone mass loss, few preventive options are available for at-risk patients, such as those with osteopenia—a condition characterized by bone mineral density (BMD) lower than normal but not severe enough to be classified as osteoporosis (16).

Osteoblasts are bone-forming cells that originate from progenitors located in the bone marrow and periosteum (17, 18). In the bone marrow, those progenitors belong to a heterogeneous population of bone marrow stromal cells (BMSCs) that contribute to bone

Author affiliations: [a]Department of Orthopaedic Surgery, University of Pennsylvania, Perelman School of Medicine, Philadelphia, PA 19104; [b]Department of Biomedical and Health Informatics, The Children's Hospital of Philadelphia, Philadelphia, PA 19104; [c]Department of Physiology and Cell Biology, University of Arkansas, School of Medicine, Little Rock, AR 72205; [d]Central Arkansas Veterans Healthcare System, John L. McClellan, Little Rock, AR 72205; and [e]Department of Oncology, University of Oxford, Division of Medical Sciences, Oxford OX37DQ, United Kingdom

Author contributions: G.L. and E. Schipani designed research; G.L., E. Sabini, D.W., and B.L. performed research; M.P.K., X.S.L., and T.B. visualization; D.W., B.L., and D.T. methodology, Visualization; A.G. conceptualization, Visualization; E. Schipani conceptualization, Funding acquisition, Investigation, Methodology, Resources, Supervision, Visualization; G.L., K.B., and D.T. analyzed data; and G.L., E. Sabini, M.P.K., X.S.L., D.W., B.L., D.T., T.B., A.G., and E. Schipani wrote the paper.

The authors declare no competing interest.

This article is a PNAS Direct Submission S.K. is a guest editor invited by the Editorial Board.

[1]G.L. and E. Sabini contributed equally to this work.

[2]To whom correspondence may be addressed. Email: ernestina.schipani@pennmedicine.upenn.edu.

This article contains supporting information online at https://www.pnas.org/lookup/suppl/doi:10.1073/pnas.2416004121/-/DCSupplemental.

Published November 27, 2024.

homeostasis and respond to external stimuli in various ways (19). Among the BMSCs, leptin receptor (*LepR*)-expressing stromal cells are considered the major source of skeletal progenitors in the adult bone marrow (19, 20).

Despite its high vascularity, the bone marrow paradoxically demonstrates an oxygen gradient, with decreasing oxygen tension originating from the peripheral endosteal regions toward the central medullary cavity (21). Interestingly, *LepR*-positive cells are found near sinusoids (20, 22, 23), suggesting their behavior may be intimately tied to the hypoxic bone marrow niche. The transcription factors hypoxia-inducible factor-1α (HIF1) and HIF2 are essential for mediating the cellular response to hypoxia (24). Under normoxic conditions, both transcription factors are degraded by the proteasome, while under hypoxic conditions they are stabilized, increasing their activity (24). HIF1 and HIF2 regulate various biological functions, enabling cells to survive, proliferate, and differentiate under hypoxia (24). Their actions can be overlapping, unique, or even opposing, depending on the cell type (25). Notably, both transcription factors are expressed in cells of the osteoblast lineage (21, 26, 27). HIF1 positively regulates bone formation, osteoblast number, and activity (26, 28), whereas HIF2 has been described as a negative regulator of bone mass accrual (29). In particular, we and others have demonstrated that the deletion of HIF2 in uncommitted osteoblast precursors during development (29, 30), but not in committed osteoprogenitors, mature osteoblasts, or osteocytes (21, 26, 31), significantly enhances bone mass by increasing bone formation and osteoblast number without affecting Bone Resorption.

Novel small molecules inhibiting HIF2 recently received FDA approval for treating Von Hippel–Lindau (*Vhl*)-related tumors showing promising results and acceptable safety profiles (32). In this study, we explored the effects of pharmacologically inhibiting HIF2 following ovariectomy as proof-of-concept that HIF2 inhibition can prevent bone loss in an estrogen deficiency model.

Results

In Vivo Loss of HIF2 in Prx1-Cre Lineage Cells Augments Trabecular Bone Mass in Female Mice. We previously demonstrated that deleting HIF2 in skeletal progenitors of the limb bud during development and their derivatives, using a *Prx1-Cre* (*Prx*) driver, markedly increases bone mass by enhancing bone formation and osteoblast numbers without affecting Bone Resorption in male mice (29). To investigate HIF2's effects on bone mass in females, we employed the same *Prx* driver for conditional HIF2 ablation (33, 34). We specifically chose this driver for consistency and to have a direct comparison between male and female mice within the same experimental framework. *Prx* transgenic mice were crossed with $Hif2^{f/f}$ mice to produce $Prx;Hif2^{f/f}$ mutants as well as $Prx;Hif2^{f/+}$ and $Hif2^{f/f}$ control littermates. In these mice, *Cre recombinase* is expressed in limb bud's cells that give rise to chondrocytes and osteoblasts in long bones and calvaria (34). As previously reported (29), $Prx;Hif2^{f/f}$ mutants were viable, born at the expected Mendelian ratio, and displayed a transient growth plate phenotype that resolved postnatally (33) (data not shown). To use the *Ai14* reporter to isolate and sort *Prx* lineage cells from mutant and control mice (see below), we generated $Prx;Hif2^{f/f};Ai14^{f/+}$ mutant mice, along with $Prx;Hif2^{f/+};Ai14^{f/+}$ and $Prx;Hif2^{+/+};Ai14^{f/+}$ controls. The *Ai14* mouse is a genetically engineered *Cre*-reporter strain which consists of a loxP-flanked STOP cassette followed by a *tdTomato* fluorescent protein sequence and is widely used to track cells in vivo (35).

At 12 wk of age, we evaluated the bone phenotypes in females only. The bones of $Prx;Hif2^{f/f};Ai14^{f/+}$ mutants showed no significant differences from those of $Prx;Hif2^{f/f}$ mutants, and similarly, there were no disparities in trabecular or cortical bone among the control groups ($Prx;Hif2^{f/+}$, $Hif2^{f/f}$, $Prx;Hif2^{f/+};Ai14^{f/+}$, $Prx;Hif2^{+/+};Ai14^{f/+}$) (SI *Appendix*, Fig. S1 *A–D*). Consequently, data from both mutant and control groups, with and without the reporter, were combined for simplicity in the final analysis and specimens indicated as $Prx;Hif2^{f/f}$, $Prx;Hif2^{f/+}$ and $Hif2^{f/f}$. $Prx;Hif2^{f/f}$ mutant mice exhibited a normal phenotype compared to control littermates, with no detectable patterning defects. Body weight, body length, and femur length of $Prx;Hif2^{f/f}$ mutant mice were virtually identical to those of $Prx;Hif2^{f/+}$ and $Hif2^{f/f}$ controls (*SI Appendix*, Fig. S1*E*).

Micro-CT analysis of femurs showed a significant increase in trabecular bone mass in $Prx;Hif2^{f/f}$ mutants compared to controls (Fig. 1 *A* and *B*). Metrics such as trabecular bone volume-to-tissue volume ratio (BV/TV), trabecular number (Tb.N.), trabecular thickness (Tb.Th.), and BMD were significantly higher in $Prx;Hif2^{f/f}$ than in $Prx;Hif2^{f/+}$ and $Hif2^{f/f}$ mice, while trabecular separation (Tb.Sp.) and bone surface-to-volume ratio (BS/BV) were significantly lower in mutants (Fig. 1*B*). Histomorphometry, limited to $Prx;Hif2^{f/f}$ mutants and $Hif2^{f/f}$ controls, as $Prx;Hif2^{f/+}$ did not differ from $Hif2^{f/f}$ by micro-CT analysis, corroborated the micro-CT data (Fig. 1 *C* and *D*, *SI Appendix*, Table S1). Notably, the number of osteoblasts relative to bone surface (N.Ob/BS), mineral surface-to-bone surface (MS/BS), mineral apposition rate (MAR), and bone formation rate per bone surface (BFR/BS) were all elevated in mutant bones relative to controls (Fig. 1*D*, *SI Appendix*, Table S1). Osteoclast counts were similar between $Hif2^{f/f}$ and $Prx;Hif2^{f/+}$ samples; however, the ratio of osteoclasts to bone surface (N.Oc./BS) was modestly reduced in $Prx;Hif2^{f/f}$ bones, reflecting an increase in bone surface due to higher bone formation rates (Fig. 1*D*, *SI Appendix*, Table S1). No obvious changes in bone marrow adiposity were observed between $Prx;Hif2^{f/f}$ mutants and $Hif2^{f/f}$ controls (Fig. 1*C*). As a result, analysis of bone marrow adiposity was not further pursued.

To investigate the potential influence of circulating factors on the observed bone phenotype, we analyzed the vertebrae (L5) from mutants and controls using micro-CT (*SI Appendix*, Fig. S2*A*). No abnormalities were detected, and no significant differences were observed between mutant mice and their littermate controls (*SI Appendix*, Fig. S2*B*). *Prx* lineage cells do not contribute to vertebrae development. This result shows that the long bone phenotype in $Prx;Hif2^{f/f}$ mutants is not attributable to changes in systemic factors.

Taken together, these data validate that HIF2 functions as an inhibitor of trabecular bone mass in female mice as well as in male mice. The observed increase in trabecular bone mass following HIF2 deletion in the *Prx* lineage primarily resulted from enhanced bone formation.

Loss of HIF2 in Prx Lineage Cells has a Modest Effect on Cortical Bone Mass in Female Mice. We have previously demonstrated that HIF2 loss results in a modest increase in cortical bone mass in male mice (29). To investigate whether similar effects occur in females, we quantified cortical parameters (*SI Appendix*, Fig. S3 and Table S1). In female mice, $Prx;Hif2^{f/f}$ mutant specimens showed a modest increase in cortical thickness (C.Th) compared to control littermates (*SI Appendix*, Fig. S3*B* and Table S1). However, there was no significant difference in the cortical area-to-total area ratio (CA/TA), polar moment of inertia (pMOI), or BMD (*SI Appendix*, Fig. S3*B* and Table S1). While pMOI was significantly higher in $Prx;Hif2^{f/+}$ mice compared to $Hif2^{f/f}$ controls (*SI Appendix*, Fig. S3*B* and Table S1), the physiological implications of these differences in pMOI remain unclear. Calcein labeling, used to assess bone formation rates, revealed no significant differences between $Prx;Hif2^{f/f}$ mutants and $Hif2^{f/f}$

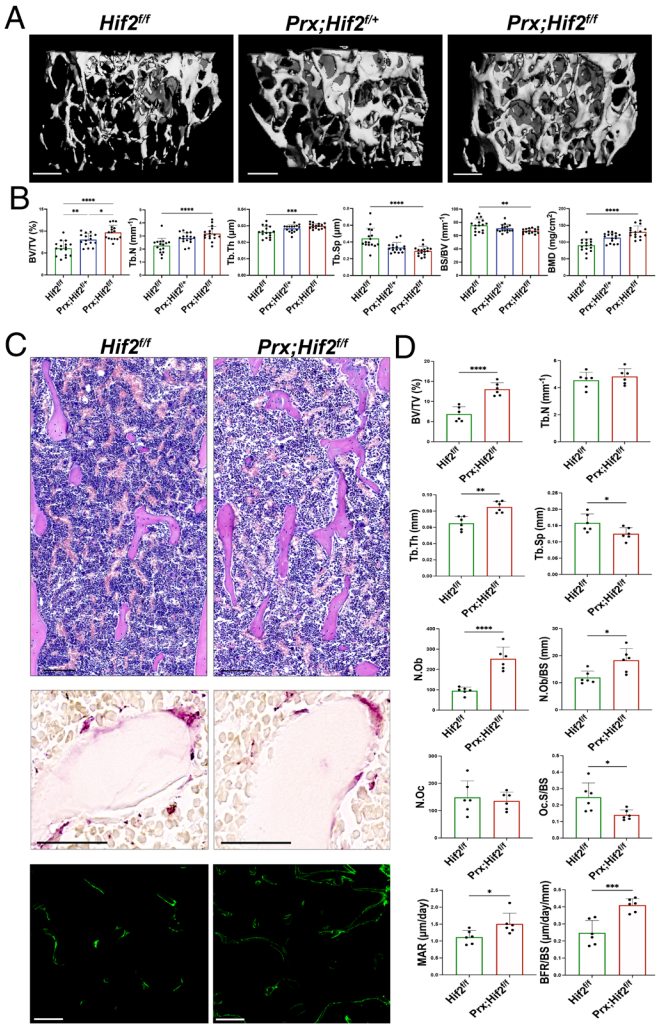

Fig. 1. Loss of HIF2 in *Prx* lineage cells augments trabecular bone mass in female mice. (*A*) Representative micro-CT 3D reconstructions of trabecular bone of femurs isolated from *Hif2*$^{f/f}$, *Prx;Hif2*$^{f/+}$ and *Prx;Hif2*$^{f/f}$ female mice at 12 wk of age. (Scale bars, 100 μm.) (*B*) Analysis of micro-CT parameters, including bone volume-to-tissue volume ratio (BV/TV), trabecular number (Tb.N), trabecular thickness (Tb.Th), trabecular spacing (Tb.Sp), bone surface-to-bone volume ratio (BS/BV), and BMD. Data are expressed as mean ± SD. *P*-value significance refers to the comparison to *Hif2*$^{f/f}$: * $P \le 0.05$, ** $P \le 0.01$, *** $P \le 0.001$, **** $P \le 0.0001$, by one-way ANOVA with multiple comparisons. (*C*) Longitudinal paraffin sections of distal femur metaphysis isolated from *Hif2*$^{f/f}$ and *Prx;Hif2*$^{f/f}$ female mice at 12 wk of age stained with hematoxylin and eosin (H&E) (*Top*) and tartrate-resistant acid phosphatase (TRAP) (*Middle*). Calcein labeling in longitudinal methylmethacrylate (MMA) sections, depicting trabecular bone at distal femur metaphysis, is shown at the *Bottom*. (Scale bar, 100 μm.) (*D*) Static and dynamic histomorphometric analysis quantifying BV/TV, Tb.N, Tb.Th, Tb.Sp, osteoblast number (N.Ob), osteoblast-to-bone surface ratio (N.Ob/BS), osteoclast number (N.Oc), osteoclast-to-bone surface ratio (N.Oc/BS), MAR, and bone formation rate-to-bone surface ratio (BFR/BS). Data are expressed as mean ± SD. *P*-value significance refers to the comparison to *Hif2*$^{f/f}$: *$P \le 0.05$, **$P \le 0.01$, ***$P \le 0.001$, ****$P \le 0.0001$, by two-tailed unpaired Student's *t*-test.

controls in cortical bone (*SI Appendix*, Fig. S3 *C* and *D*, Table S1). Taken together, our results suggest that as in male mice, the loss of HIF2 in *Prx* lineage cells impacts trabecular bone mass more significantly than cortical bone mass also in female mice.

Loss of HIF2 in Prx Lineage Cells Expands the Pool of Skeletal Progenitors. Previous studies have demonstrated that the loss of HIF2 in osteoblasts does not significantly affect bone mass, unlike its effect in skeletal progenitors (21, 26). This suggests a distinct role for HIF2 in skeletal progenitors. To explore this possibility, we performed unbiased single-cell RNA-sequencing (scRNA-seq) analysis on bone marrow *Prx* lineage cells from 7-wk-old female *Prx;Hif2*$^{f/f}$*;Ai14*$^{f/+}$ mutant and *Prx;Hif2*$^{+/+}$*;Ai14*$^{f/+}$ control mice. The cells were sorted using flow cytometry, based on their *tdTomato* expression (*SI Appendix*, Fig. S4*A*), and the assay was performed in biological duplicates. The analysis revealed 12 distinct cell clusters (Fig. 2*A*). Uniform manifold approximation and projection (UMAP) representation displayed a similar cluster distribution between control and mutant groups (*SI Appendix*, Fig. S4*B*). Despite sorting cells with the Ai14 reporter driven by *Prx*, hematopoietic, and endothelial cells, identified by *Ptprc (CD45)* and *Pecam 1* (*CD31*) mRNA expression respectively, were detected in the sorted population (*SI Appendix*, Fig. S4*C*).

Cluster 7 emerged as particularly significant, expressing *Hif2* mRNA alongside skeletal progenitor markers such as leptin receptor (*LepR*) (Fig. 2*B*), paired related homeobox 1 (*Prrx1*), and platelet-derived growth factor receptor alpha (*Pdgfra*) mRNAs (*SI Appendix*, Fig. S4*D*) (20, 36). A few cells in this cluster also expressed classical markers of early stages of osteoblast commitment and differentiation such as collagen type I alpha 1 (*Col1a1*), runt-related transcription factor 2 (*Runx2*), and osterix *(Sp7)* mRNAs, whereas osteocalcin (*Ocn*) mRNA, a marker of terminally differentiated osteoblasts, was barely detectable (*SI Appendix*, Fig. S4*D*).

Most notably, Cluster 7 was expanded in *Prx;Hif2*$^{f/f}$*;Ai14*$^{f/+}$ mutants, constituting a larger proportion of the total cell population (7.82%) compared to controls (2.44%) (Fig. 2*C*). However, the substantial difference in cluster size between mutants and controls limited detailed analysis of differentially expressed genes.

We then complemented the in vivo data with an in vitro assay. BMSCs were isolated from *Hif2*$^{f/f}$ and *Prx;Hif2*$^{f/f}$ mice, expanded in vitro, replated, and cultured under either normoxic (20% O_2) or hypoxic (1% O_2) conditions. It is important to note that these oxygen levels are arbitrary selections since bone and bone marrow are vascularized tissues that typically experience cyclical oxygen fluctuations, not steady-state hypoxia. qPCR of 2-LoxP genomic DNA confirmed efficient recombination of the floxed allele in mutant cells (deletion efficiency: 78% ± 0.08 SEM) (Fig. 3*A*). As expected, these cells expressed *LepR* mRNA in both *Hif2*$^{f/f}$ and *Prx;Hif2*$^{f/f}$(Fig. 3*B*).

Notably, qRT-PCR analysis of total RNA after 7 d in culture revealed no significant difference in *Runx2* mRNA expression between mutants and controls, either in normoxia or hypoxia (Fig. 3*B*). However, *Col1a1* mRNA expression was modestly higher in *Prx;Hif2*$^{f/f}$ BMSCs compared to controls under normoxic condition (Fig. 3*B)*. More importantly, osteopontin/secreted phosphoprotein (*Spp1*), Sp7, and alkaline phosphatase (*Alpl*) mRNA levels were significantly increased in *Prx;Hif2*$^{f/f}$ BMSCs cultured under hypoxic conditions compared to controls (Fig. 3*B). Runx2, Col1a1, SSP1, Sp7, and Alpl* mRNAs are all markers of the early stage of osteoblast differentiation.

Cell counts and Trypan blue exclusion tests for cell viability were also performed on BMSCs after 7 d in culture. The total cell number was significantly higher in *Prx;Hif2*$^{f/f}$ cultures compared to controls, which had fewer viable cells and more dead cells both under normoxic and hypoxic conditions (Fig. 3*C*). Last, double-stranded DNA (dsDNA) levels were quantified over various time points (2 to 11 d after seeding). The dsDNA content was significantly elevated in *Prx;Hif2*$^{f/f}$ cultures compared to controls across all time points both under 20% O_2 and 1% O_2 conditions (Fig. 3*D*).

In summary, these findings indicate that the loss of HIF2 in the *Prx* lineage expands the pool of skeletal progenitors independently of oxygen levels. This expansion is likely due to increased proliferation, though reduced cell death may also play a role, and is not associated to impaired differentiation of progenitors into osteoblasts. Notably, under hypoxia, osteoblast differentiation

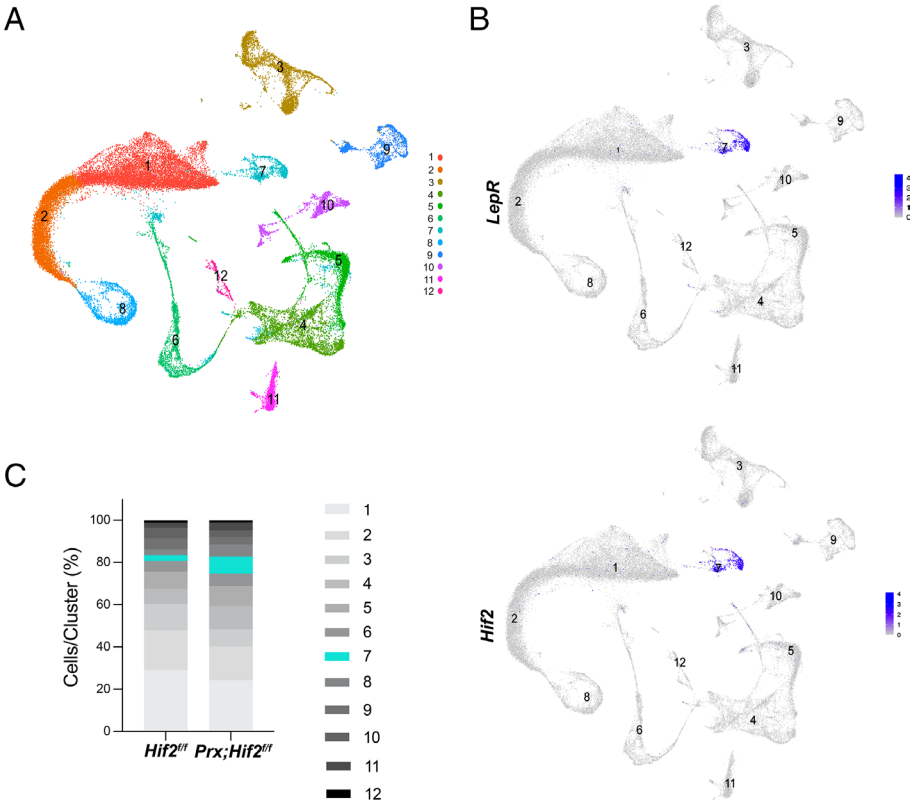

Fig. 2. Single Cell RNA-Sequencing analysis of *Prx* lineage cells isolated from the bone marrow of *Prx;Hif2*$^{+/+}$*;Ai14*$^{f/+}$ and *Prx;Hif2*$^{f/f}$*;Ai14*$^{f/+}$. (*A*) UMAP visualization of aggregate clusters. (*B*) UMAP visualization of the leptin receptor (*LepR*) and hypoxia-inducible factor 2 (*Hif2*). (*C*) A bar graph comparing the percentage of cells/cluster in *Prx;Hif2*$^{+/+}$*;Ai14*$^{f/+}$ versus *Prx;Hif2*$^{f/f}$*;Ai14*$^{f/+}$. Cluster 7 enriched in skeletal progenitor markers is highlighted in red.

appears to be modestly enhanced, as indicated by higher levels of *Sp7*, *Spp1*, and *Alpl* mRNAs in mutant hypoxic cells.

Pharmacological Inhibition of HIF2 Prevents Trabecular Bone Loss Following Ovariectomy. Next, we explored the therapeutic potential of targeting HIF2 in preventing trabecular bone loss following ovariectomy. For this purpose, we investigated the efficacy of available HIF2 inhibitors.

HIF2 inhibitors are small molecules which act on the HIF2 Per-ARNT-Sim (PAS)-B domain to prevent the formation of the necessary heterodimer complex for downstream activity. They have been recently approved by the FDA for the treatment of clear cell renal cell carcinoma (ccRCC) (32, 37). Given the role of HIF2 as a negative regulator of trabecular bone mass, we hypothesized that inhibiting HIF2 could represent a translational approach to prevent bone loss in experimental models of postmenopausal osteoporosis.

We administered the inhibitor PT2399 (32, 38) at two dosages—100 mg/kg/d (high dose) and 60 mg/kg/d(low dose), respectively. In an initial experiment, 26 adult female FVB/N mice, 8 wk old, were ovariectomized (OVX) or sham-operated (Sham) and then randomized to receive either 50 mg/kg PT2399 or a vehicle (Veh) twice daily by oral gavage. Observations from this cohort showed no effects of high doses of PT2399 on Sham mice, leading us to exclude this experimental group in the subsequent investigations.

In a second experiment, we grouped mice into three categories: Veh-Sham, Veh-OVX, and PT2399-OVX. Treatments were administered at 30 mg/kg twice daily for five consecutive days with a subsequent 2-d washout. In both experiments, we initiated treatment 1 wk postsurgery, with the effects on trabecular bone mass evaluated 5 wk later (Fig. 4*A*). The Veh-Sham and Veh-OVX mice from both studies were indistinguishable in terms of experimental procedure, allowing their results to be combined in the final bone phenotype analysis (Fig. 4).

At the outset of the study (Week 0), there were no significant differences in body weight across groups. By weeks 3 and 6, OVX mice displayed a significant increase in body weight compared to sham-operated mice, irrespective of treatment (Fig. 4*A*). This increase was consistent with menopausal conditions (39), which also led to significant uterine atrophy, independent of the treatment (Fig. 4*A*).

Micro-CT analysis of the femurs revealed that Veh-OVX exhibited expected reductions in trabecular bone mass compared to the control group (Veh-Sham), characterized by decreased BV/TV, Tb.N., and BMD, and increased Tb.Sp and BS/BV (Fig. 4 *B* and *C*). In contrast, PT2399-treated OVX mice showed significantly higher BV/TV, Tb.N, and BMD, and lower Tb.Sp and BS/BV compared to Veh-OVX mice (Fig. 4*C*). Crucially, there was no detectable difference between PT2399-treated OVX mice and Veh-Sham mice, indicating that PT2399, even at lower doses, fully prevented the loss of trabecular bone mass induced by ovariectomy (Fig. 4 *B* and *C*).

Micro-CT analysis of L5 vertebra produced findings consistent with those observed in femoral assessments (Fig. 4 *D* and *E*). Quantitative analysis of trabecular parameters demonstrated significant reductions in BV/TV, Tb.N, Tb.Th, and BMD in Veh-OVX mice compared to Veh-Sham mice (Fig. 4*E*). Correspondingly, Tb.Sp and BS/BV were significantly increased in the Veh-OVX group (Fig. 4*E*). Similarly to the results in femurs, administration of high doses of PT2399 effectively countered the loss of trabecular bone, showing no significant differences in trabecular parameters between PT2399-OVX mice and Veh-Sham mice (Fig. 4*E*). The low-dose regimen of PT2399 notably mitigated the OVX-induced

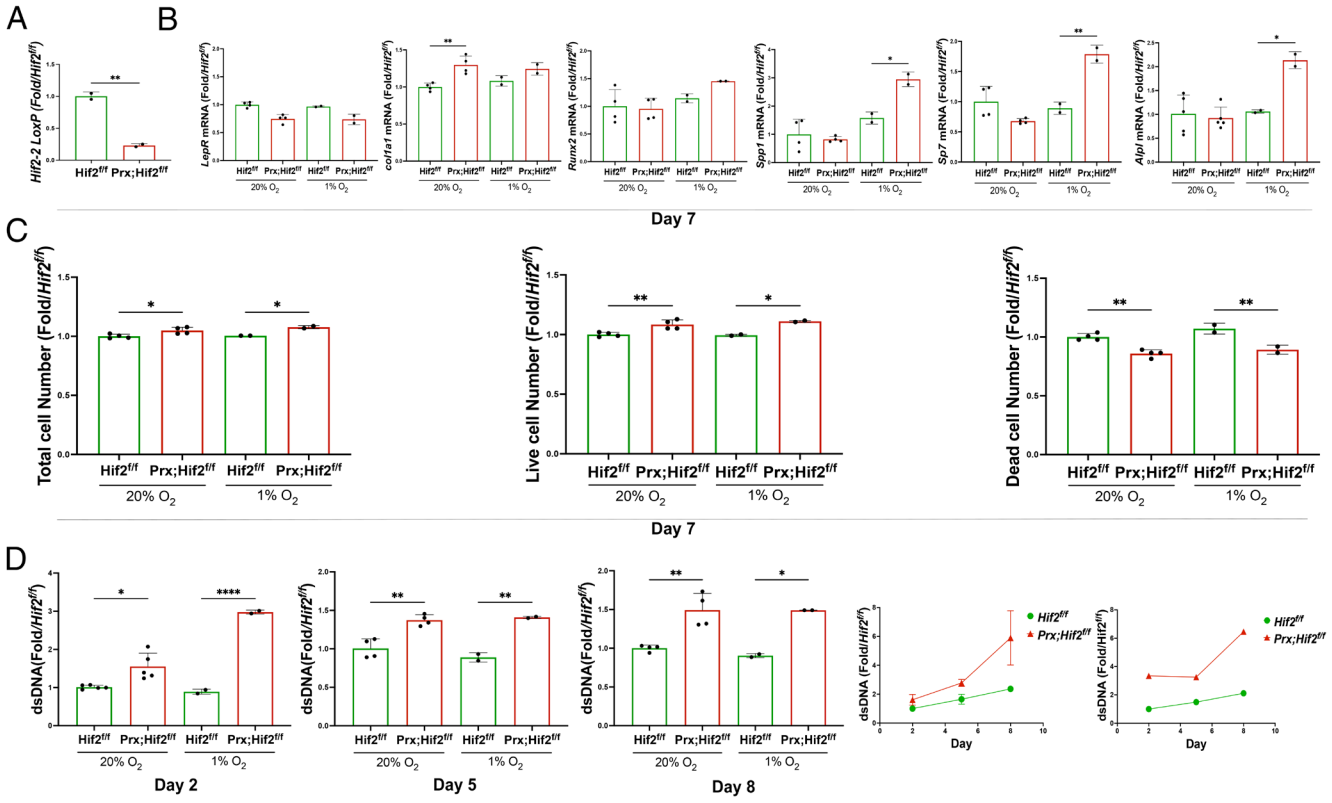

Fig. 3. Loss of HIF2 in the *Prx* lineage increases the number of skeletal proliferative cells in vitro. (*A*) *2*-LoxP qPCR was performed on genomic DNA extracted from *Hif2*$^{f/f}$ and *Prx;Hif2*$^{f/f}$ BMSC upon a brief in vitro culture. Data were normalized to Von Hippel–Lindau (*Vhl*) as internal reference for genomic DNA. (*B*) qRT-PCR of total RNA isolated from *Hif2*$^{f/f}$ and *Prx;Hif2*$^{f/f}$ BMSCs either in normoxia (20% O_2) or hypoxia (1% O_2). Data were normalized to the expression of TATA-binding protein (*Tbp*) mRNA. *LepR*, leptin receptor; *Col1a1*, collagen type I alpha 1; *Runx2,* runt-related transcription factor 2; *Spp1,* osteopontin/secreted phosphoprotein-1; *Sp7*, Osterix; *Alpl,* alkaline phosphatase. (*C*) Cell counting with Trypan blue exclusion of *Hif2*$^{f/f}$ and *Prx;Hif2*$^{f/f}$ BMSCs in normoxia (20% O_2) or hypoxia (1% O_2). (*D*) Double-stranded DNA (dsDNA) levels were quantified in BMSCs from *Hif2*$^{f/f}$ and *Prx;Hif2*$^{f/f}$ mice over various time points (2 to 8 d after seeding) either in normoxia (20% O_2) or hypoxia (1% O_2). Data are expressed as mean ± SD. *P*-value significance refers to the comparison to *Hif2*$^{f/f}$: **P* ≤ 0.05, ***P* ≤ 0.01, ****P* ≤ 0.001, **** *P* ≤ 0.0001, by two-tailed unpaired Student's *t*-test. All the experiments were performed in biological and technical duplicates or triplicates.

reductions in Tb.Th and BMD, as well as the increases in Tb.Sp and BS/BV (Fig. 4*E*). However, the improvement in BV/TV and Tb.N was dose-dependent, with low doses (60 mg/kg/d) of PT2399 not quite as effective as the high-dose (100 mg/kg/d) treatment (Fig. 4*E*).

Given the consistent bone loss observed in both femurs and vertebrae postovariectomy histomorphometry was selectively performed on femurs. This analysis confirmed the micro-CT findings (Fig. 5 and *SI Appendix*, Table S2). Notably, Oc.N/BS did not differ between groups, while Ob.N/BS was significantly lower in Veh-OVX mice compared to Veh-Sham mice (Fig. 5*B* and *SI Appendix*, Table S2). This reduction was effectively prevented by PT2399 administration either at low or high doses (Fig. 5*B* and *SI Appendix*, Table S2). As in the genetic experiment, no obvious changes in bone marrow adiposity were observed (Fig. 5*A*).

Double calcein labeling revealed a significant increase in MAR and BFR/BS in PT2399-treated OVX mice compared to Veh-OVX mice, matching levels observed in the control group (Fig. 5*B* and *SI Appendix*, Table S2). This leads us to conclude that PT2399 mitigates bone loss, at least in part, through enhancing bone formation, corroborated by the increased Ob.N/BS in PT2399-OVX mice when compared to Veh-OVX.

Increase in Bone Resorption is well characterized in low bone mass diseases due to estrogen deficiency (1, 6); however, some studies in animal models, including ours, showed no detectable differences in osteoclast numbers following ovariectomy (40) (Fig. 5*B* and *SI Appendix*, Table S2). This discrepancy is most likely due to the time interval between ovariectomy and bone analysis.

Collectively, our in vivo studies demonstrate that PT2399 effectively prevents trabecular bone loss induced by ovariectomy in mice at both low and high doses. A key mechanism appears to be stimulation of bone formation, consistent with the observed phenotypes following HIF2 loss in the *Prx* lineage. However, since HIF2 presence in osteoclasts has been documented and genetic ablation of HIF2 in these cells is known to increase bone mass (30), PT2399's ability to prevent bone loss may also involve an inhibitory effect on Bone Resorption, likely through a direct impact on osteoclasts.

Limited Impact of Ovariectomy on Cortical Bone. Cortical bone parameters were also evaluated using micro-CT and dynamic histomorphometry (*SI Appendix*, Fig. S5 and Table S2). Notably, Ps.MAR significantly decreased in Veh-OVX mice, a reduction that was effectively mitigated by PT2399-treatment (*SI Appendix*, Fig. S5*B* and Table S2). However, all other cortical parameters remained unchanged across the groups, suggesting that ovariectomy does not significantly influence cortical bone at least at the time points we evaluated (*SI Appendix*, Fig. S5*B* and Table S2).

This observation is consistent with existing literature that identifies trabecular bone as the primary site affected by postmenopausal osteoporosis, particularly during the early stages of the disease (41). Given the negligible impact of ovariectomy on cortical bone, and consequently the minimal effects of PT2399 on this bone type even at high dosages, further analysis of cortical bone following treatment with low doses of PT2399 was deemed unnecessary.

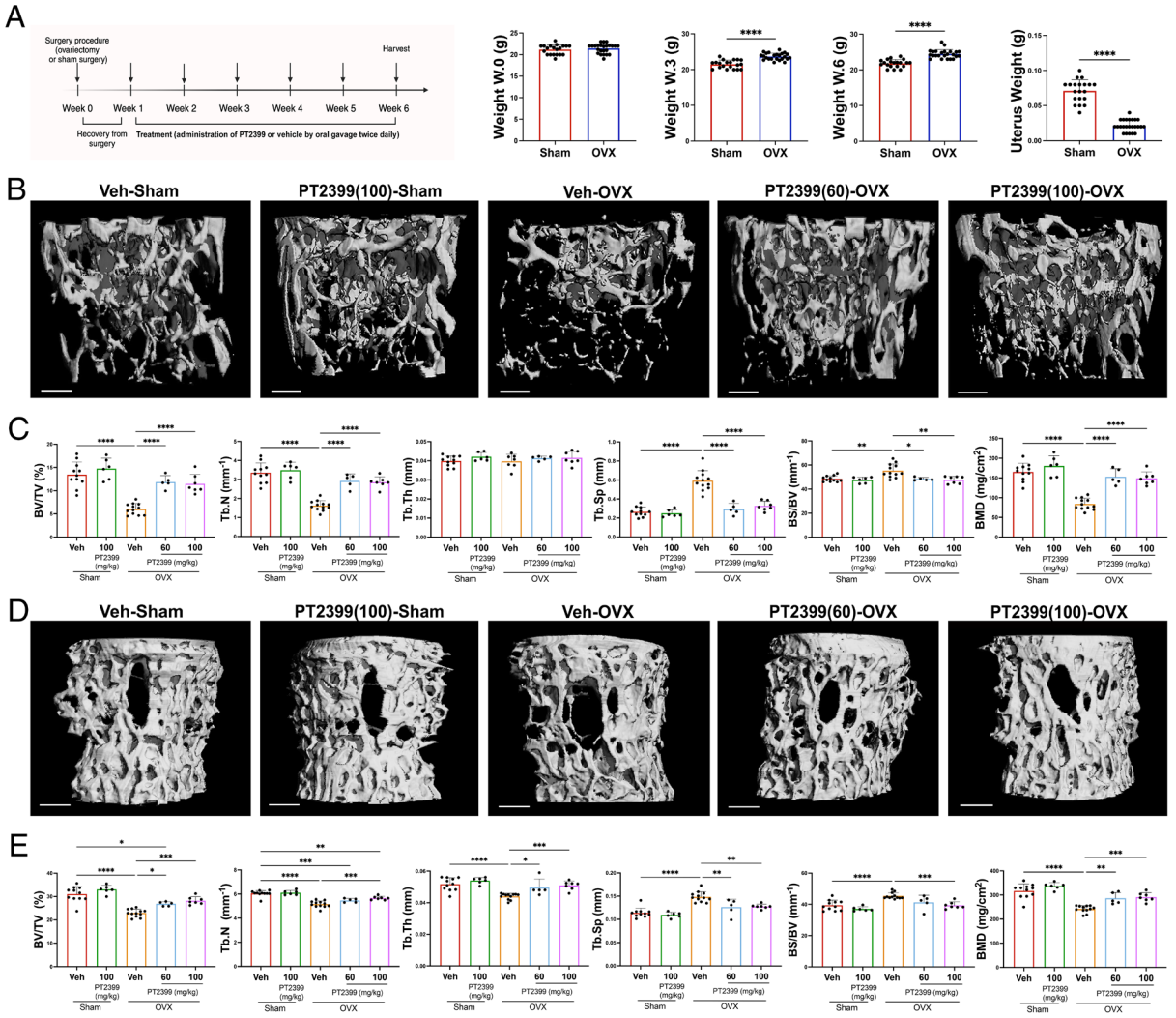

Fig. 4. PT2399 fully prevents the loss of trabecular bone mass due to ovariectomy as shown by micro-CT analysis. (*A*) The scheme of oral PT2399 treatment regimen is provided on the *Left*. Analysis of morphometric parameters, including body weight at weeks 0,3 and 6, and uterus weight at the end of the study, is shown on the right. Data are expressed as mean ± SD. *P*-value significance refers to the comparison to the Veh-Sham group: $*P \le 0.05$, $**P \le 0.01$, $***P \le 0.001$, $***P \le 0.0001$, by two-tailed unpaired Student's *t*-test. (*B*) Representative micro-CT 3D reconstructions of trabecular bone of femurs isolated from OVX or sham-operated wild-type FVB/N mice treated with low (60 mg/kg/d) or high (100 mg/kg/d) doses of PT2399 or vehicle. (*C*) Quantification of micro-CT parameters including bone volume-to-tissue volume ratio (BV/TV), trabecular number (Tb.N), trabecular thickness (Tb.Th), trabecular spacing (Tb.Sp), bone surface-to-bone volume ratio (BS/BV), and BMD. (*D*) Representative micro-CT 3D reconstruction of trabecular bone of vertebral bodies (L5) isolated from OVX or sham-operated mice treated with low (60 mg/kg/d) or high (100 mg/kg/d) doses of PT2399 or vehicle. (*E*) Quantification of BV/TV, Tb.N, Tb.Th, Tb.Sp, BS/BV, and BMD. Data are expressed as mean ± SD. *P*-value significance refers to the comparison to the Veh-Sham group: $*P \le 0.05$, $**P \le 0.01$, $***P \le 0.001$, $****P \le 0.0001$, by one-way ANOVA with multiple comparisons.

PT2399 Negatively Impacts Erythropoiesis. The safety profile of PT2399 was also evaluated. Mice appeared grossly normal with no signs of morbidity under all treatment conditions. Although PT2399 treatment did not cause severe systemic toxicities, aligning with findings from prior studies (32), the twice-daily oral administration of high-dose PT2399 led to a modest reduction in hemoglobin (HGB) and hematocrit (HCT) levels (Fig. 6 *A* and *B*). Furthermore, red blood cells (RBC), mean corpuscular volume (MCV), and mean corpuscular hemoglobin (MCH) were significantly reduced in mice treated with high doses of PT2399 (Fig. 6 *C* to *E*). These adverse effects are likely due to diminished renal erythropoietin (EPO) production, a direct downstream target of HIF2 (42).

Indeed, EPO serum levels were significantly decreased in mice treated with high doses of PT2399 (Fig. 6*G*). The low-dose regimen mitigated the decreases in Hb, Hct, RBC, and EPO, showing significant differences in Hb, Hct, and EPO between mice treated with low doses of PT2399 and those receiving high doses (Fig. 6 *A*, *B* and *G*). Moreover, no significant differences in MCV and MCH were observed between mice treated with the low-dose regimen and those given the vehicle (Fig. 6 *D* and *E*). Thus, PT2399 treatment led to a dose-dependent reduction in EPO levels, with the most significant decrease observed at the higher dose.

PT2399 Expands the Pool of Skeletal Proliferative Cells In Vitro. PT2399-OVX mice show increased Ob.N, MAR, BFR/BS, consistent with the augmented trabecular bone mass due to HIF2 loss in *Prx* lineage cells. Previous studies have shown that HIF2 loss in committed osteoprogenitors, mature osteoblasts, or osteocytes does not significantly alter bone mass (21, 26, 31). Taken together, these data point to PT2399's specific impact on skeletal progenitors. To explore this, BMSCs were isolated from 8-wk-old female FVB/N wild-type mice and cultured under normoxic (20% O2) or hypoxic (1% O2) conditions with PT2399 treatments at concentrations of 2 μM, 10 μM, and 20 μM in dimethyl sulfoxide (DMSO), or with vehicle (DMSO) for 7 d.

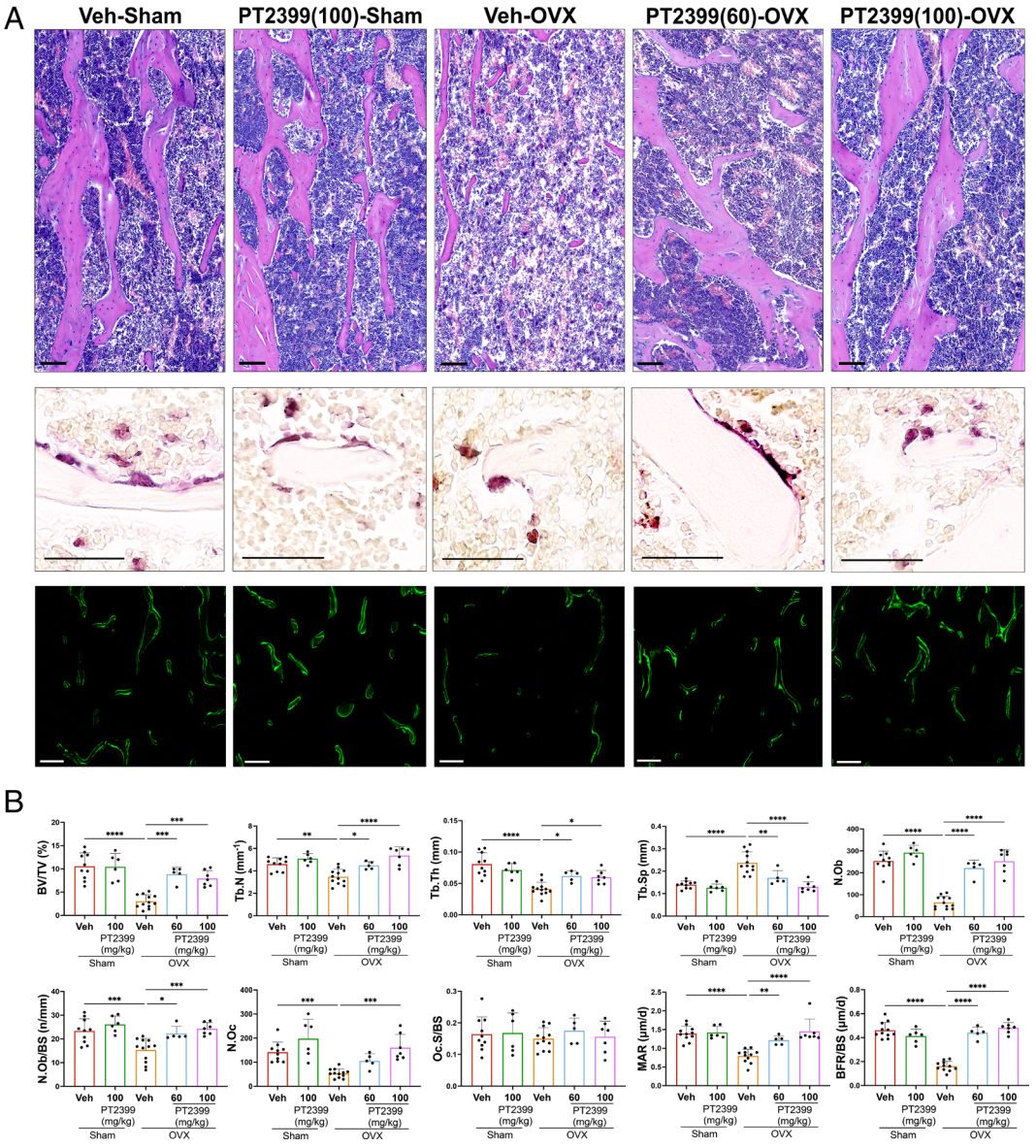

Fig. 5. An increase in bone formation promotes the preventive effect of PT2399 on trabecular bone loss upon ovariectomy. (*A*) Longitudinal paraffin sections stained with H&E (*Top*), and tartrate-resistant acid phosphatase (TRAP) (*Middle*) of distal femur metaphysis isolated from OVX or sham-operated wild-type FVB/N mice treated with low (60 mg/kg/d) or high (100 mg/kg/d) doses of PT2399 or vehicle. Calcein labeling in longitudinal MMA unstained sections, depicting trabecular bone at distal femur metaphysis, is shown at the *Bottom*. (Scale bar, 100 µm.) (*B*) Static and dynamic histomorphometric analysis quantifying bone volume-to-tissue volume ratio (BV/TV), trabecular number (Tb.N), trabecular thickness (Tb.Th), trabecular spacing (Tb.Sp), osteoblast number (N.Ob), osteoblast-to-bone surface ratio (N.Ob/BS), osteoclast number (N.Oc), osteoclast-to-bone surface ratio (N.Oc/BS), MAR, and BFR/BS. Data are expressed as mean ± SD. *P*-value significance refers to the comparison to the Veh-Sham group: **P*≤ 0.05, ***P* ≤ 0.01, ****P* ≤ 0.001, *****P* ≤ 0.0001, by one-way ANOVA with multiple comparisons.

qRT-PCR analysis of total RNA from BMSCs cultured for 7 d revealed that hypoxia-induced increases in osteoprotegerin (*Opg*), N-myc downstream-regulated gene 1 (*Ndrg1*), and SRY-Box Transcription Factor 9 (*Sox9*) mRNAs—known downstream targets of HIF2 (21, 29, 38)—were significantly suppressed by PT2399 in a dose-dependent manner (Fig. 7*A*). Vascular endothelial growth factor-A (*Vegfa*) mRNA expression served as a positive control to validate the hypoxic conditions (Fig. 7*A*). Consistent with the notion that hypoxia stabilizes both HIF1 and HIF2 and *Vegfa* mRNA is a downstream target of both (24, 43), its expression was not significantly altered by PT2399 treatment (Fig. 7*A*). The markers of the early stages of osteoblast differentiation were also investigated. Expression of *Alpl* mRNA was modestly decreased by PT2399 (20 µm) in hypoxic conditions while levels of *Col1a1*, *Runx2*, *Sp7*, and *Spp1*mRNAs were virtually unaffected by the treatment under either normoxia or hypoxia (Fig. 7*B*).

Cell counting and Trypan blue exclusion tests for cell viability were also performed on BMSCs isolated and treated with 10 µM and 20 µM of PT2399 as described previously. The total number of cells was significantly higher in the PT2399-treated BMSCs compared to those treated with vehicle, both under normoxic and hypoxic conditions, with no significant difference observed between the two concentrations (Fig. 7*C*). Furthermore, PT2399 treatment resulted in a notable decrease in the number of dead cells and an increase in the number of viable cells under both normoxic and hypoxic conditions (Fig. 7*C*).

To corroborate these findings, dsDNA levels were measured in BMSCs treated with 10 or 20 µM of PT2399 or vehicle across various time points (1 to 8 d posttreatment initiation) (Fig. 7*D*). The dsDNA content was significantly elevated in the PT2399-treated groups compared to the vehicle-treated groups on days 5 and 8 under both 20% and 1% O_2 conditions (Fig. 7*D*).

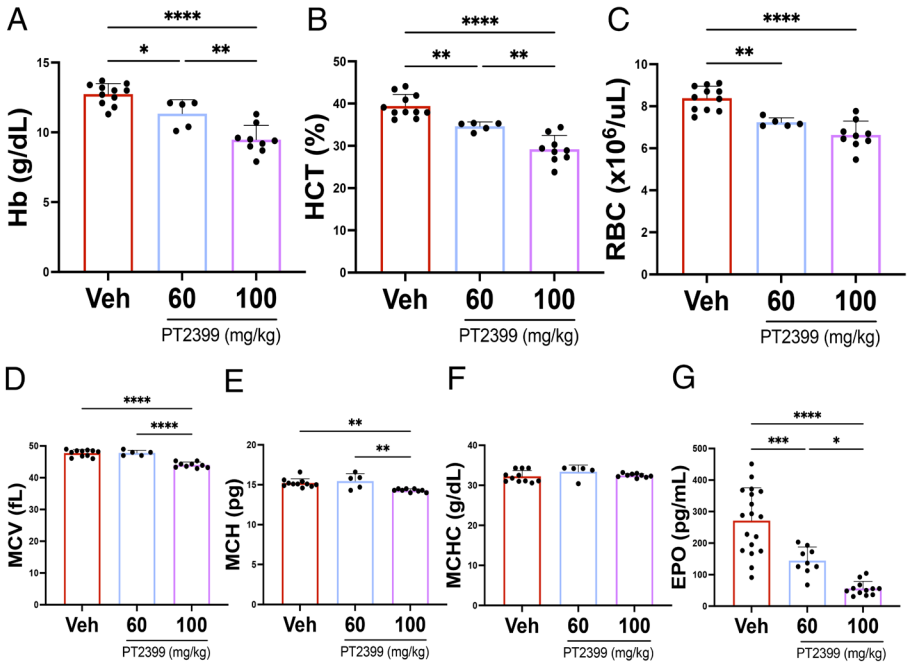

Fig. 6. PT2399 negatively affects erythropoiesis. Complete blood count (CBC) analysis of OVX or sham-operated wild-type FVB/N mice treated with low (60 mg/kg/d) or high (100 mg/kg/d) doses of PT2399 or vehicle. (*A*) Hb, hemoglobin. (*B*) HCT, hematocrit. (*C*) RBC, red blood cells. (*D*) MCV, mean corpuscular volume. (*E*) MCH, mean corpuscular hemoglobin. (*F*) MCHC, mean corpuscular hemoglobin concentration. (*G*) EPO, erythropoietin. Data are expressed as mean ± SD. *P*-value significance refers to the comparison to the Veh-Sham group: **P* ≤ 0.05; ***P* ≤ 0.01; ****P* ≤ 0.001; *****P* ≤ 0.0001 by one-way ANOVA with multiple comparisons.

Next, we further investigated the impact of PT2399 on terminally differentiated osteoblasts. BMSCs were isolated as above. Cells were initially cultured for 15 d. Subsequently, treatments with 10 μM and 20 μM of PT2399 in DMSO, or with vehicle, were administered under normoxic or hypoxic conditions, and the cells were cultured for an additional seven days. The hypoxia-induced increase in *Ndrg1* mRNA was significantly reduced by PT2399 in a dose-dependent manner. Moreover, the expression levels of *Opg*, and *Sox9* mRNAs were significantly reduced by PT2399 under both normoxic and hypoxic conditions, confirming PT2399's direct impact on BMSCs in vitro (*SI Appendix*, Fig. S6 *A–C*). Notably, PT2399 reduced the hypoxia-dependent increase in mRNA expression of receptor activator of nuclear factor kappa-B ligand (*RankL*) (*SI Appendix*, Fig. S6*D*). However, it had no effect on the mRNA levels of *Alpl* and osteocalcin (*Ocn)* (*SI Appendix*, Fig. S6 *E* and *F*). *Alpl* is expressed throughout the lifespan of osteoblastic cells, while *Ocn* is exclusively produced by terminally differentiated osteoblasts.

To address whether the effect of PT2399 on bone skeletal proliferative cells in vitro was unique to the model employed or applicable to other models, we isolated BMSCs from 16-mo-old wild-type C57BL/6 mice. Cells were expanded in vitro, replated, and treated with 10 μM and 20 μM of PT2399 in DMSO, or with vehicle under normoxic (20% O_2) or hypoxic (1% O_2) conditions for 7 d. The hypoxia-induced increase in *Ndrg1, Sox9, and Opg* mRNA was significantly reduced by PT2399 (*SI Appendix*, Fig. S7*A*). While the treatment had no effect on the mRNA levels of *Col1a1, Runx2, Spp1, Sp7,* and *Alpl* (*SI Appendix*, Fig. S7*B*), the total number of cells was significantly higher in the PT2399-treated BMSCs compared to those treated with vehicle, under both 20% and 1% O_2 conditions (*SI Appendix*, Fig. S7*C*). This increase is likely due to the higher number in live cells, as there was no difference in dead cell number in PT2399-treated BMSCs compared to those treated with vehicle (*SI Appendix*, Fig. S7*C*). Consistently, the dsDNA content was significantly increased by PT2399 on days 5 and 8 under both 20% and 1% O_2 conditions (*SI Appendix*, Fig. S7*D*).

In summary, PT2399 treatment expands the pool of skeletal progenitors without inhibiting or promoting their differentiation into osteoblasts in either young or aged BMSCs under either normoxic or hypoxic conditions. Therefore, our data support a model in which PT2399 treatment increases the number of progenitors through promoting proliferation and reducing cell death but without directly influencing their differentiation.

Discussion

Low-bone mass diseases typically result from an imbalance between osteoclast-mediated Bone Resorption and osteoblast-mediated bone formation. Previously, we reported that the genetic loss of HIF2 in skeletal progenitors of the limb bud and their descendants during development increases bone mass by promoting bone formation (29). Since this effect was solely investigated in male mice, it remained uncertain whether intrinsic gender-based differences exist in HIF2's role in regulating bone mass. In the current study, we demonstrate that HIF2 deficiency has the same effect in female mice. These data indicate that the effect of HIF2 loss in skeletal progenitors and their derivatives is not influenced by gender.

Of note, the increase in cortical bone mass was modest in both male and female *Prx;Hif2*^{fff} mutant mice (29). The findings corroborate the hypothesis that trabecular and cortical bone are distinct compartments (44).

The increase in trabecular bone mass following HIF2 deletion in skeletal progenitors of the limb bud and their derivatives was secondary to enhanced bone formation associated with increased osteoblast number, without a concomitant increase in Bone Resorption. As discussed earlier, HIF2 deficiency in committed osteoprogenitors, mature osteoblasts, or osteocytes did not significantly enhance bone mass (21, 26, 31), indicating that HIF2 has a unique role in skeletal progenitors. Along those lines, the loss of HIF2 in the *LepR*-positive population has been found to prevent radiation-induced bone loss through the enhancement of bone

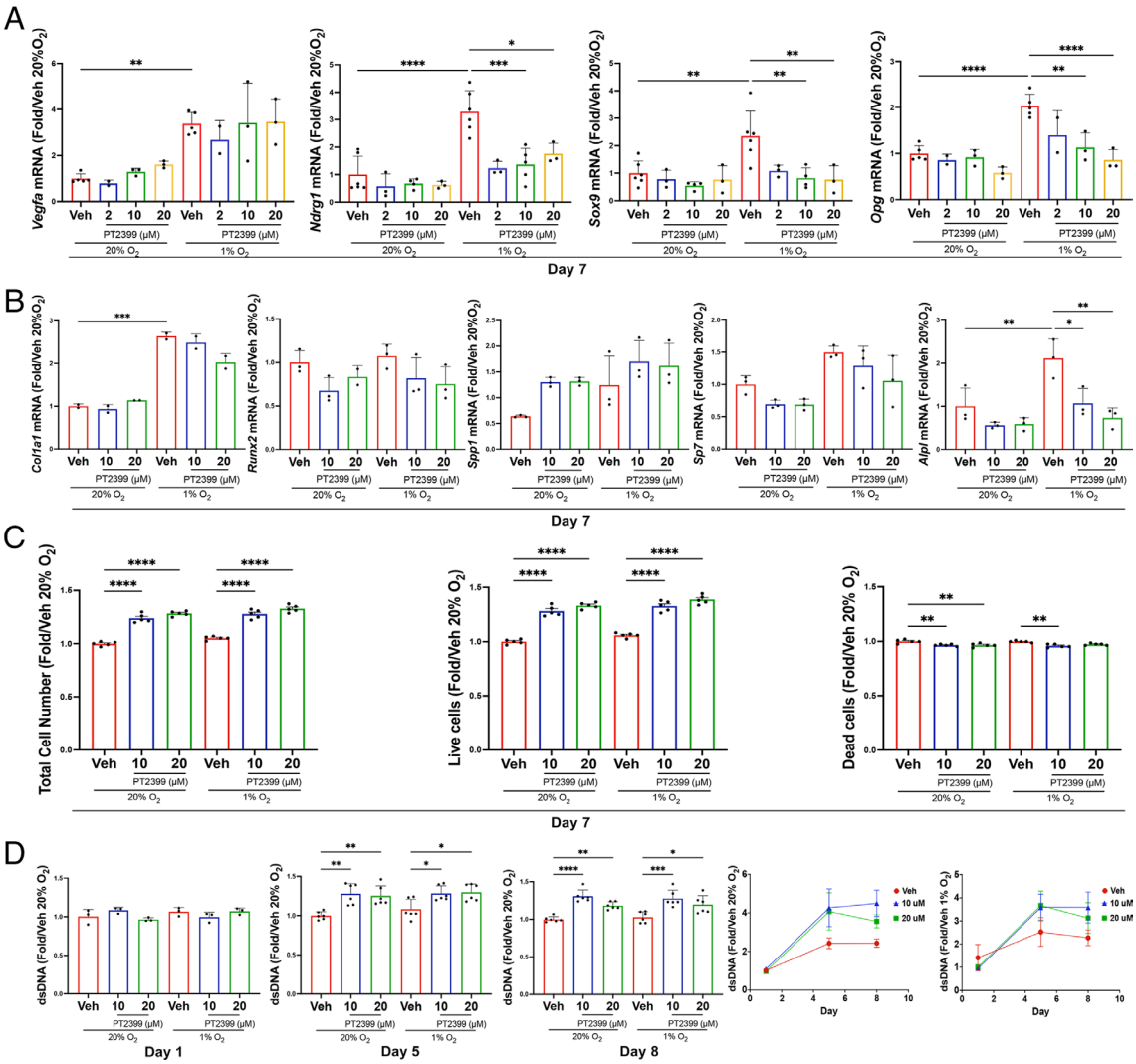

Fig. 7. PT2399 has a direct effect on BMSC in vitro. (*A* and *B*) qRT-PCR of total RNA isolated from wild-type FVB/N BMSC treated with PT2399 at the indicated concentration, or vehicle (DMSO), either in normoxia (20% O_2) or hypoxia (1% O_2), for 7 d. Data were normalized to the expression of TATA-binding protein (*Tbp*) mRNA. *Vegfa*, vascular endothelial growth factor-A; *Ndrg1*, N-myc downstream-regulated gene 1; *Sox9*, SRY-Box Transcription Factor 9; *Opg*, osteoprotegerin; *Col1a1*, collagen type I alpha 1; *Runx2*, runt-related transcription factor 2; *Spp1*, osteopontin/secreted phosphoprotein-1; *Sp7*, Osterix; *Alpl*, alkaline phosphatase. (*C*) Cell counting with Trypan blue exclusion of wild-type FVB/N BMSCs treated with PT2399 at the indicated concentration, or vehicle (DMSO), either in normoxia (20% O_2) or hypoxia (1% O_2), for 7 d. (*D*) Double-stranded DNA (dsDNA) measurement in wild-type FVB/N BMSCs treated with PT2399 at the indicated concentration and time points, or vehicle (DMSO), either in normoxia (20% O_2) or hypoxia (1% O_2). Data are expressed as mean ± SD. *P*-value significance refers to the comparison to the vehicle in normoxic condition: $*P \le 0.05$, $**P \le 0.01$, $***P \le 0.001$, $****P \le 0.0001$, by ANOVA with multiple comparisons. All the experiments were performed in biological and technical duplicates or triplicates.

formation (45). Moreover, our scRNA-seq experiments showed a unique expansion of the skeletal progenitor population identified by the expression of *LepR* mRNA. Consistently, our in vitro assays demonstrated that loss of HIF2 within *Prx* lineage boosts the pool of *LepR*-positive skeletal proliferative cells without promoting their osteoblastic differentiation. Taken together, these findings suggest that the augmented bone formation observed in *Prx;Hif2*$^{f/f}$ mutant mice is due to an increase in osteoblast number secondary to an expansion of the skeletal progenitor population, rather than by an augmentation of osteoblast activity.

Interestingly, in our scRNA-seq, *Hif2* mRNA, which is often present in endothelial cells (46, 47), was not expressed in cells expressing *Pecam* mRNA, an established marker of endothelial cells (48, 49). The biological significance of these findings remains to be established.

Since HIF2 is a key regulator of bone homeostasis, we hypothesize that HIF2 could be evaluated as a target for treating low bone mass diseases, including estrogen deficiency conditions such as postmenopausal osteoporosis. Our hypothesis is supported by published reports indicating that OVX-induced bone loss was alleviated by the universal loss of HIF2 (30). Moreover, treatment with the HIF2 inhibitor PT2399 was sufficient to prevent the decrease in bone mass in a single-limb irradiation mouse model (45). Our study provides proof-of-concept that pharmacological inhibition of HIF2 fully prevents bone loss, even at low doses, in an experimental model of estrogen deficiency—a context that has not been previously explored.

We tested the HIF2 inhibitor PT2399 in ovariectomized mice at 8 wk of age, a commonly used model of estrogen deficiency (50–54). Although postmenopausal women are older than 8 wk-old mice, estrogen deficiency also induces bone loss in younger females, such as those with premature ovarian insufficiency (4, 5), and the degree of bone loss depends on the condition and timing of analysis and treatment. We selected 8 wk-old mice based on existing literature to demonstrate that PT2399 can prevent bone loss in an estrogen-deficient model. However, these mice may not have reached peak bone mass, particularly in the FVB/N strain, and the model may not fully replicate human conditions.

Further studies are needed to determine whether PT2399 can also reverse bone loss and to assess its efficacy in older mice. Despite these limitations, our proof-of-concept study opens broad avenues for understanding HIF2's role in estrogen-related bone mass regulation.

Unlike the genetic experiment, PT2399 administration results in a systemic inhibition of HIF2. It has been reported that HIF2 is also expressed in osteoclasts, and osteoclast-specific knockout of HIF2 increases bone mass by reducing osteoclast number under homeostatic conditions (30). Therefore, it is possible that the prevention of trabecular bone loss upon ovariectomy by PT2399 is due to both an enhancement of bone formation and a reduction in Bone Resorption.

Interestingly, PT2399 expands the pool of *LepR*-positive skeletal proliferative cells in vitro, at least in part by reducing cell death. This finding mirrors the expansion of the *LepR*-positive population observed in the bone marrow of *Prx;Hif2*$^{f/f}$. Importantly, PT2399 does not affect bone mass in sham-operated mice. This finding supports the concept that *LepR*-progenitors are quiescent in the adult, although they can rapidly proliferate and give origin to osteoblasts when stimulated, highlighting their potential in therapeutic strategies (19, 20, 55). Indeed, loss of HIF2 in *LepR*-positive population has been shown to not affect bone mass under homeostatic conditions despite its preventive effect on bone loss upon radiation (45). On the other hand, in our study, PT2399 was administered for only 5 wk. The short treatment period might have contributed to the absence of an overt phenotype in sham-operated mice.

The role of the hypoxia signaling pathway in general, and HIF2 in particular, in modulating the biology of stem/progenitor cells appears to be cell-context dependent (56, 57). HIF2 has been described as an oncoprotein in *Vhl*-deficient ccRCC (58, 59), and its inhibition may help control cell growth in cancer models. Paradoxically, elevated expression of HIF2 in other cell lines led to cell cycle arrest (60), suggesting that the role of HIF2 may be cell-type specific, with its impact on cell proliferation and cell death varying depending on the experimental conditions.

Our experimental evidence suggests that either genetic or pharmacological inhibition of HIF2 expands the pool of skeletal progenitors in the bone marrow. This expansion contributes to the augmentation of bone mass through an increase in osteoblast number. Notably, this expansion occurs both in normoxia and hypoxia, which indicates HIF2 serves biological roles that go beyond the hypoxic response, as we have previously reported (29).

While PT2399 treatment expands the pool of skeletal progenitors, we have no experimental evidence that it directly inhibits or promotes their differentiation into osteoblasts in either young or aged BMSCs under normoxic or hypoxic conditions.

Genetic loss of HIF2 expands skeletal progenitors, independent of oxygen levels, without impairing osteoblast differentiation. Under hypoxia, this loss modestly enhances osteoblast differentiation, as seen by increased Sp7, Spp1, and Alpl mRNA expression, even with unchanged Runx2 levels. This aligns with prior findings that HIF2 blocks the transition from Runx2-positive to Sp7-expressing cells (29). These hypoxia-specific results highlight the bone marrow microenvironment's role in cell fate. The difference between PT2399 treatment and genetic HIF2 inhibition may stem from full HIF2 loss in the genetic model versus incomplete inhibition in the pharmacological model, leading to distinct outcomes.

One significant drawback of HIF2 inhibitor therapy is the potential normal tissue effects excluding bone. Approximately 90% of cancer patients receiving a HIF2 inhibitor experience anemia due to the loss of HIF2 which is needed for renal EPO production (32). As expected, we observed modest anemia in mice given PT2399 compared to those receiving vehicle. However, the low-dose regimen significantly mitigated the decrease in Hb, Hct, and RBC and circulating EPO, while preserving the treatment's effectiveness in preventing bone loss.

Notably, HIF2 is critical for the regulation of iron homeostasis by regulating the expression of the divalent metal transporter 1 (DMT1) and Duodenal cytochrome B (DCYTB) in the duodenum (61). Given the decrease in MCV and MCH upon administration of high doses of PT2399, in principle the occurrence of anemia could be in part contributed, at least at high doses, by iron deficiency. However, since PT2399 treatment leads to a dose-dependent reduction in EPO levels that aligns with the CBC data, this indicates that reduced EPO expression is the major driver of anemia in PT2399-treated mice.

We have previously reported that osteoblastic cells produce and secrete EPO in a HIF2-dependent manner (27). We have also shown that the loss of EPO in skeletal progenitors of the limb bud and their descendants does not affect bone mass (62). Therefore, it is highly unlikely that genetic or pharmacological inhibition of HIF2 augments trabecular bone mass by inhibiting the production of osteoblastic EPO.

Interestingly, circulating EPO negatively impacts bone mass accrual and homeostasis through direct effects on bone cells (63–66). Therefore, in principle, a reduction in circulating levels of EPO could contribute to the preventive effect of PT2399 on bone loss upon ovariectomy. However, experimental evidence does not support this conclusion. First, the genetic loss of HIF2 in skeletal progenitors of the limb bud and their descendants increases bone mass without affecting circulating levels of EPO (29). Second, targeting PT2399 to the bone marrow through nanoparticle technology preserves the protective effect of the drug against radiation-induced bone loss (45). Third, iron-deficient anemia has been associated to low bone mass phenotypes (67). Notably, in our experimental model, PT2399 protects bone mass despite the presence of anemia. Last, and more importantly, low doses of PT2399 were as effective as high doses in preventing bone mass loss following ovariectomy. Since low doses of PT2399 led to reductions in EPO, Hb, Hct, and RBC that were significantly less pronounced compared to those observed with higher doses, this indicates that the protective effect of PT2399 on bone mass is independent of its impact on EPO production. Thus, our findings indicate that it is possible to leverage the bone-protective effects of PT2399 while minimizing adverse hematological outcomes by optimizing the dosage.

In conclusion, the genetic loss of HIF2 in skeletal progenitors increases trabecular bone mass primarily through enhanced bone formation. Pharmacological inhibition of HIF2 positively affects bone mass in adult bone, independently of any putative action of this transcription factor during development. Specifically, the HIF2 inhibitor PT2399 is sufficient to completely prevent the occurrence of osteoporosis in an estrogen deficiency model, opening a broad avenue for the treatment of low bone mass conditions caused by estrogen deficiency. The expansion of the *LepR*-positive population in *Prx;Hif2*$^{f/f}$ mice, the increase in osteoblast number in these mutants, as well as in OVX mice treated with PT2399, and the increase in cell number observed in skeletal proliferative cells treated in vitro with PT2399, all indicate that the inhibition of HIF2 boosts the expansion of skeletal progenitors. This expansion ultimately leads to an increase in both osteoblast number and bone formation, resulting in higher trabecular bone mass.

Further studies will be also directed to establish whether the effects of PT2399 on trabecular bone mass can be entirely uncoupled from those on EPO production. Alternatively, it will be important to investigate whether specifically targeting HIF2

inhibitors to bone preserves their positive effects on bone mass while preventing anemia.

Materials and Methods

Detailed methods are provided in *SI Appendix, Material and Methods*.

Data, Materials, and Software Availability. scRNAseq data have been deposited in NCBI's Gene Expression Omnibus GEO series accession GSE263228 (https://www.ncbi.nlm.nih.gov/geo/query/acc.cgi?acc=GSE263228) (68). All other data are included in the manuscript and/or *SI Appendix*.

ACKNOWLEDGMENTS. We thank the Penn Cytomics and Cell Sorting Shared Resource Laboratory at the University of Pennsylvania (P30 016520), the Histology and Micro-CT Cores at Umich (NIH P30 AR069620), and at UPenn (NIH P30 AR069619) for their excellent technical support. This study was supported by NIH R01 AR073022-01A1 to Ernestina Schipani.

1. R. Eastell *et al.*, Postmenopausal osteoporosis. *Nat. Rev. Dis. Primers* **2**, 16069 (2016).
2. S. R. Cummings, L. J. Melton, Epidemiology and outcomes of osteoporotic fractures. *Lancet* **359**, 1761–1767 (2002).
3. A. C. Looker, L. G. Borrud, B. Dawson-Hughes, J. A. Shepherd, N. C. Wright, Osteoporosis or low bone mass at the femur neck or lumbar spine in older adults: United States, 2005–2008. *NCHS Data Brief* **93**, 1–8 (2012).
4. A. R. Jones *et al.*, Bone health in women with premature ovarian insufficiency/early menopause: A 23-year longitudinal analysis. *Hum. Reprod.* **39**, 1013–1022 (2024).
5. V. B. Popat *et al.*, Bone mineral density in estrogen-deficient young women. *J. Clin. Endocrinol. Metab.* **94**, 2277–2283 (2009).
6. P. Garnero, E. Sornay-Rendu, M. C. Chapuy, P. D. Delmas, Increased bone turnover in late postmenopausal women is a major determinant of osteoporosis. *J. Bone Miner Res.* **11**, 337–349 (1996).
7. T. J. Martin, N. A. Sims, RANKL/OPG; Critical role in bone physiology. *Rev. Endocr. Metab. Disord* **16**, 131–139 (2015).
8. S. C. Manolagas, C. A. O'Brien, M. Almeida, The role of estrogen and androgen receptors in bone health and disease. *Nat. Rev. Endocrinol.* **9**, 699–712 (2013).
9. M. N. Weitzmann, R. Pacifici, Estrogen deficiency and bone loss: An inflammatory tale. *J. Clin. Invest.* **116**, 1186–1194 (2006).
10. S. Gera *et al.*, First-in-class humanized FSH blocking antibody targets bone and fat. *Proc. Natl. Acad. Sci. U.S.A.* **117**, 28971–28979 (2020).
11. L. Sun *et al.*, FSH directly regulates bone mass. *Cell* **125**, 247–260 (2006).
12. S. H. Tella, J. C. Gallagher, Prevention and treatment of postmenopausal osteoporosis. *J. Steroid Biochem. Mol. Biol.* **142**, 155–170 (2014).
13. R. Eastell *et al.*, Pharmacological management of osteoporosis in postmenopausal women: An endocrine society* clinical practice guideline. *J. Clin. Endocrinol. Metab.* **104**, 1595–1622 (2019).
14. K. G. Saag *et al.*, Romosozumab or alendronate for fracture prevention in women with osteoporosis. *N. Engl. J. Med.* **377**, 1417–1427 (2017).
15. T. J. Martin, N. A. Sims, E. Seeman, Physiological and pharmacological roles of PTH and PTHrP in bone using their shared receptor, PTH1R. *Endocr. reviews* **42**, 383–406 (2021).
16. F. Cosman *et al.*, Clinician's guide to prevention and treatment of osteoporosis. *Osteoporos Int.* **25**, 2359–2381 (2014).
17. D. Trompet, S. Melis, A. S. Chagin, C. Maes, Skeletal stem and progenitor cells in bone development and repair. *J. Bone Miner Res.* **39**, 633–654 (2024), 10.1093/jbmr/zjae069.
18. K. Nakashima *et al.*, The novel zinc finger-containing transcription factor osterix is required for osteoblast differentiation and bone formation. *Cell* **108**, 17–29 (2002).
19. E. C. Jeffery, T. L. A. Mann, J. A. Pool, Z. Zhao, S. J. Morrison, Bone marrow and periosteal skeletal stem/progenitor cells make distinct contributions to bone maintenance and repair. *Cell Stem Cell* **29**, 1547–1561.e1546 (2022).
20. B. O. Zhou, R. Yue, M. M. Murphy, J. G. Peyer, S. J. Morrison, Leptin-receptor-expressing mesenchymal stromal cells represent the main source of bone formed by adult bone marrow. *Cell Stem. Cell* **15**, 154–168 (2014).
21. C. Wu *et al.*, Oxygen-sensing PHDs regulate bone homeostasis through the modulation of osteoprotegerin. *Genes. Dev.* **29**, 817–831 (2015).
22. T. H. Ambrosi *et al.*, Distinct skeletal stem cell types orchestrate long bone skeletogenesis. *Elife* **10**, e66063 (2021).
23. J. A. Spencer *et al.*, Direct measurement of local oxygen concentration in the bone marrow of live animals. *Nature* **508**, 269–273 (2014).
24. G. L. Semenza, Hypoxia-inducible factors in physiology and medicine. *Cell* **148**, 399–408 (2012).
25. B. Keith, R. S. Johnson, M. C. Simon, HIF1alpha and HIF2alpha: Sibling rivalry in hypoxic tumour growth and progression. *Nat. Rev. Cancer* **12**, 9–22 (2011).
26. S. H. Shomento *et al.*, Hypoxia-inducible factors 1alpha and 2alpha exert both distinct and overlapping functions in long bone development. *J. Cell Biochem.* **109**, 196–204 (2010).
27. E. B. Rankin *et al.*, The HIF signaling pathway in osteoblasts directly modulates erythropoiesis through the production of EPO. *Cell* **149**, 63–74 (2012).
28. J. N. Regan *et al.*, Up-regulation of glycolytic metabolism is required for HIF1alpha-driven bone formation. *Proc. Natl. Acad. Sci. U.S.A.* **111**, 8673–8678 (2014).
29. C. Merceron *et al.*, Hypoxia-inducible factor 2alpha is a negative regulator of osteoblastogenesis and bone mass accrual. *Bone Res.* **7**, 7 (2019).
30. S. Y. Lee *et al.*, Controlling hypoxia-inducible factor-2alpha is critical for maintaining bone homeostasis in mice. *Bone Res.* **7**, 14 (2019).
31. S. V. Mendoza *et al.*, Degradation-resistant hypoxia inducible factor-2alpha in murine osteocytes promotes a high bone mass phenotype. *JBMR Plus* **7**, e10724 (2023).
32. W. Chen *et al.*, Targeting renal cell carcinoma with a HIF-2 antagonist. *Nature* **539**, 112–117 (2016).
33. E. Araldi, R. Khatri, A. J. Giaccia, M. C. Simon, E. Schipani, Lack of HIF-2alpha in limb bud mesenchyme causes a modest and transient delay of endochondral bone development. *Nat. Med.* **17**, 25–26 (2011).
34. M. Logan *et al.*, Expression of Cre Recombinase in the developing mouse limb bud driven by a Prxl enhancer. *Genesis* **33**, 77–80 (2002).
35. L. Madisen *et al.*, A robust and high-throughput Cre reporting and characterization system for the whole mouse brain. *Nat. Neurosci.* **13**, 133–140 (2010).
36. R. M. Farahani, M. Xaymardan, Platelet-derived growth factor receptor alpha as a marker of mesenchymal stem cells in development and stem cell biology. *Stem. Cells Int.* **2015**, 362753 (2015).
37. E. Jonasch *et al.*, Belzutifan for renal cell carcinoma in von hippel–lindau disease. *N. Engl. J. Med.* **385**, 2036–2046 (2021).
38. H. Cho *et al.*, On-target efficacy of a HIF-2alpha antagonist in preclinical kidney cancer models. *Nature* **539**, 107–111 (2016).
39. G. A. Greendale *et al.*, Changes in body composition and weight during the menopause transition. *JCI Insight* **4**, e124865 (2019).
40. F. Jehan *et al.*, New insights into the role of matrix metalloproteinase 3 (MMP3) in bone. *FASEB Bioadv.* **4**, 524–538 (2022).
41. B. L. Riggs *et al.*, A population-based assessment of rates of bone loss at multiple skeletal sites: Evidence for substantial trabecular bone loss in young adult women and men. *J. Bone Miner Res.* **23**, 205–214 (2008).
42. T. Souma, N. Suzuki, M. Yamamoto, Renal erythropoietin-producing cells in health and disease. *Front Physiol.* **6**, 167 (2015).
43. E. Aro *et al.*, Hypoxia-inducible factor-1 (HIF-1) but not HIF-2 is essential for hypoxic induction of collagen prolyl 4-hydroxylases in primary newborn mouse epiphyseal growth plate chondrocytes. *J. Biol. Chem.* **287**, 37134–37144 (2012).
44. L. Calvi *et al.*, Activation of the PTH/PTHrP receptor in osteoblastic cells has differential effects on cortical and trabecular bone. *J. Clin. Invest.* **107**, 277–286 (2001).
45. W. Guo *et al.*, Radiation-induced bone loss in mice is ameliorated by inhibition of HIF-2alpha in skeletal progenitor cells. *Sci. Transl. Med.* **15**, eabo5217 (2023).
46. H. Tian, S. L. McKnight, D. W. Russell, Endothelial PAS domain protein 1 (EPAS1), a transcription factor selectively expressed in endothelial cells. *Genes. Dev.* **11**, 72–82 (1997).
47. M. S. Wiesener *et al.*, Widespread hypoxia-inducible expression of HIF-2alpha in distinct cell populations of different organs. *FASEB J.* **17**, 271–273 (2003).
48. P. J. Newman, The biology of PECAM-1. *J. Clin. Invest.* **100**, S25–S29 (1997).
49. P. J. Newman *et al.*, PECAM-1 (CD31) cloning and relation to adhesion molecules of the immunoglobulin gene superfamily. *Science* **247**, 1219–1222 (1990).
50. S. Lucas *et al.*, Short-chain fatty acids regulate systemic bone mass and protect from pathological bone loss. *Nat. Commun.* **9**, 55 (2018).
51. L. Lin *et al.*, SIRT2 regulates extracellular vesicle-mediated liver-bone communication. *Nat. Metab.* **5**, 821–841 (2023).
52. Y. Zhang, L. Wei, R. J. Miron, B. Shi, Z. Bian, Anabolic bone formation via a site-specific bone-targeting delivery system by interfering with semaphorin 4D expression. *J. Bone Miner Res.* **30**, 286–296 (2015).
53. X. X. Guo *et al.*, Prevention of osteoporosis in mice after ovariectomy via allograft of microencapsulated ovarian cells. *Anat. Rec. (Hoboken)* **293**, 200–207 (2010).
54. S. Zhou *et al.*, Age-dependent variations of cancellous bone in response to ovariectomy in C57BL/6J mice. *Exp. Ther. Med.* **15**, 3623–3632 (2018).
55. Y. Matsushita *et al.*, Bone marrow endosteal stem cells dictate active osteogenesis and aggressive tumorigenesis. *Nat. Commun.* **14**, 2383 (2023).
56. J. Mazumdar *et al.*, O2 regulates stem cells through Wnt/beta-catenin signalling. *Nat. Cell Biol.* **12**, 1007–1013 (2010).
57. K. E. Lee, M. C. Simon, From stem cells to cancer stem cells: HIF takes the stage. *Curr. Opin. Cell Biol.* **24**, 232–235 (2012).
58. A. Elorza *et al.*, HIF2alpha acts as an mTORC1 activator through the amino acid carrier SLC7A5. *Mol. Cell* **48**, 681–691 (2012).
59. H. Doan *et al.*, HIF-mediated Suppression of DEPTOR Confers Resistance to mTOR Kinase Inhibition in Renal Cancer. *iScience* **21**, 509–520 (2019).
60. T. Hackenbeck *et al.*, HIF-1 or HIF-2 induction is sufficient to achieve cell cycle arrest in NIH3T3 mouse fibroblasts independent from hypoxia. *Cell Cycle* **8**, 1386–1395 (2009).
61. M. Mastrogiannaki *et al.*, HIF-2alpha, but not HIF-1alpha, promotes iron absorption in mice. *J. Clin. Invest.* **119**, 1159–1166 (2009).
62. G. Lanzolla *et al.*, Osteoblastic erythropoietin is not required for bone mass accrual. *JBMR Plus* **8**, ziae052 (2024).
63. S. Hiram-Bab *et al.*, Erythropoietin directly stimulates osteoclast precursors and induces bone loss. *Faseb J.* **29**, 1890–1900 (2015).
64. M. Rauner *et al.*, Epo/EpoR signaling in osteoprogenitor cells is essential for bone homeostasis and Epo-induced bone loss. *Bone Res.* **9**, 42 (2021).
65. M. Rauner *et al.*, Increased EPO levels are associated with bone loss in mice lacking PHD2 in EPO-producing cells. *J. Bone Miner Res.* **31**, 1877–1887 (2016).
66. S. Suresh, J. Lee, C. T. Noguchi, Erythropoietin signaling in osteoblasts is required for normal bone formation and for bone loss during erythropoietin-stimulated erythropoiesis. *Faseb J.* **34**, 11685–11697 (2020).
67. M. G. Ledesma-Colunga *et al.*, Shaping the bone through iron and iron-related proteins. *Semin. Hematol.* **58**, 188–200 (2021).
68. G. Lanzolla, E. Sabini, E. Schipani, NCBI's Gene Expression Omnibus GEO series accession GSE263228. Single cell RNA sequencing of mutant bone marrow stromal cells lacking HIF2 and controls. NCBI Gene Expression Omnibus. https://www.ncbi.nlm.nih.gov/geo/query/acc.cgi?acc=GSE263228. Deposited 4 April 2024.